

SUPPLEMENTAL MATERIAL

I. Material and Methods

Reagents. Adenosine diphosphate (ADP) was purchased from Chrono-log (Havertown, PA), human- α -thrombin was purchased from Enzyme Research Laboratory (South Bend, IN), anti-TLR2, TLR6, TLR7, TLR9, and IRAK antibodies were purchased from Cell Signaling Technology (Danvers, MA), AbCam (Cambridge, MA), Millipore (Billerica, MA), eBioscience (San Diego, CA) and Hycult biotechnology b.v. (Canton, MA). AKT and phospho-AKT(Ser473) antibodies were purchased from Cell Signaling Technology (Danvers, MA). Human and murine TLR2, TLR4, TLR6, and TLR9 agonists, as well as specific blocking agents were purchased from InvivoGen (San Diego, CA) and Imgenex (San Diego, CA). The Fab fragments of TLR antibodies were generated by pepsin digestion using Pierce Fab micro preparation kit, Thermo-Scientific (Rockford, IL). Conjugated anti-murine P-selectin and anti-murine activated integrin- $\alpha_{IIb}\beta_3$ (clone JON/A) monoclonal antibodies were purchased from Emfret Analytics (GmbH & Co. KG, Eibelstadt, Germany). FACS grade and fluorochrome conjugated specific anti-human P-selectin mouse monoclonal antibody and PAC-1 were purchased from BD Biosciences (San Jose, CA). The HEK-Blue™ hTLR9 cells co-expressing human TLR9 and an NF- κ B-inducible *SEAP* (secreted embryonic alkaline phosphatase) reporter gene and the control cells HEK-Blue™ Null expressing only the NF- κ B-inducible *SEAP* were purchased from InvivoGen™ (San Diego, CA). Functional grade human full-length TLR9 recombinant protein without tag, and human TLR9 (AAH32713, 99 a.a. - 215 a.a.) partial recombinant protein with a ~26kD N-terminal GST tag were purchased from Novus Biologicals LLC (Littleton, CO), for SPR assays and ELISA. Ly294-002 was purchased from Sigma-Aldrich, PP2 and Bay 61 were purchased from EMD-Milipore Inc, (Billerica, MA) and all other reagents were from Sigma-Aldrich (St. Louis, MO), unless otherwise specified.

Experimental Animals. Wild type (WT), MyD88^{-/-}, TLR2^{-/-}, and SR-BI^{-/-} mice were purchased from Jackson Laboratories (Bar Harbor, ME). CD36^{-/-} animals were generated as described.¹ TLR9^{-/-} and TLR6^{-/-} mice were purchased from Oriental Yeast Co., Ltd (Tokyo, Japan). All strains were at least 99% C57Bl/6 background. WT and knockout mice were used between 10 and 14 weeks of age. Animals were housed in ventilated cages with ad libitum access to food and water, on a 14:10 light dark cycle. All animal procedures were approved prior to the study by the Institutional Animal Care and Use Committee of Cleveland Clinic.

Preparation of ω -Carboxyethylpyrrole-modified Peptide and Proteins.² Paal-Knorr reactions of γ -dicarbonyl compounds with primary amines provided an efficient route to 2-(ω -carboxyalkyl)pyrroles.³ Syntheses of γ -ketoaldehydes, 4,7-dioxoheptanoic acid (DOHA), and its phosphatidylcholine ester (DOHA-PC) were developed to allow unambiguous production of 2-(ω -carboxyethyl)pyrrole (CEP) and the corresponding PC ester. First, a Grignard reagent was produced from 2-(2-bromoethyl)-1,3-dioxolane, followed by selective acylation of this organomagnesium derivative with 3-carbomethoxypropionyl chloride. Saponification of the resulting ethylene ketal keto ester delivered a carboxylic acid that, when coupled with 2-lysophosphatidylcholine in the presence of dicyclohexylcarbodiimide and *N,N*-dimethylaminopyridine, gave a stable precursor that yielded DOHA-PC upon hydrolysis. Transketalization of the ethylene ketal with acetone provided a mixture containing DOHA, presumably in equilibrium with the corresponding hemiacetal based on the ¹H NMR spectrum that exhibits two aldehydic hydrogen singlets. Paal-Knorr condensation of DOHA or DOHA-PC with the dipeptide acetyl-Gly-Lys-*O*-methyl ester generated the CEP-dipeptides, DOHA-dipeptide, or CEP-PC-

dipeptide that were fully characterized by ^1H NMR.⁴ ^1H NMR and ^{13}C NMR spectra were recorded at 300 and 75 MHz, respectively, and solvents and chromatography conditions for purification of synthetic products were as described elsewhere.⁴ As mentioned earlier, Paal-Knorr condensation with DOHA was used to prepare CEP-modified keyhole limpet hemocyanin (CEP-KLH), bovine serum albumin (CEP-BSA), human serum albumin (CEP-HSA), and glyceraldehyde-3-phosphate dehydrogenase (CEP-GPDH). All reactions in an inert atmosphere were under argon unless otherwise specified. Protein concentrations were determined using the Pierce bicinchoninic acid protein assay,⁵ and pyrrole concentrations were determined using the Ehrlich reagent, and the above CEP-dipeptide as a reference standard.⁶

Preparation of Anti-CEP Antibodies. A *Pasteurella*-free, New Zealand White rabbit was inoculated subcutaneously along the back and rear legs with about 340 μg (<7.1 nmol) of CEP-KLH (<1 mol of pyrrole/mol of KLH, 2.7 mg/ml KLH in PBS). Initial injections were administered with Freund's complete adjuvant, and booster injections were given every 21 days with incomplete Freund's adjuvant. Antibody titers were monitored 10 days after each inoculation by ELISA. The rabbit was exsanguinated after 92 days and a total of 5 inoculations. The IgG fraction of anti-CEP antibodies was purified using immobilized protein G.⁷

Measuring CEP concentration in plasma/platelets by competitive ELISA. 96-well ELISA plates (Costar Corp.) were coated with CEP-BSA solution in PBS (220nM) overnight at 4°C. The plates were then washed three times with PBS and blocked with 2% BSA for 1 hour at 37°C. Meanwhile, pre-incubate the CEP standard, Plasma, or platelet lysate with anti-CEP rabbit polyclonal antibody at 37°C for 1 hour. The supernatant of antibody-antigen complex were then added to the 96-well and incubate at room temperature for 1 hour followed by goat-anti rabbit IgG-HRP secondary antibody (Invitrogen, 1:3000) at room temperature. The plate was then washed 3 times with PBST, 100 μL of ABTS (Invitrogen) solution was added into the wells, incubated for 30 minutes at 37°C and then data were acquired at 405 nm with microplate reader.

Isolation of platelets. Informed consent was obtained from donors in accordance with the Declaration of Helsinki. Human venous blood was drawn from healthy donors into acid-citrate-dextrose (ACD; 85mM tri-sodium citrate, 65mM citric acid, and 111mM D-glucose, pH 4.6) solution, PGI₂ (1 $\mu\text{g}/\text{mL}$) and apyrase 0.02U/mL. ACD solution with 1 $\mu\text{g}/\text{mL}$ PGI₂ was used as an anticoagulant for platelet isolation by gel-filtration. In murine studies, blood was drawn from the inferior vena cava of anesthetized mice into a syringe containing 3.8% sodium citrate for aggregation experiments using platelet rich plasma (PRP). PRP and gel-filtered platelets were isolated as described.⁸ Platelet counts were assessed by a Cellometer™ Auto-M10 (Nexcelom Bioscience Lawrence, MA).

Immunomagnetic separation of leukocytes from platelet rich plasma. Human platelets used for detecting Toll-like receptor expression were further processed according to manufacturer's protocol (Miltineyi Biotec) by incubating PRP with anti-human CD45 pan-leukocyte antibody tagged with magnetic beads and passed through while blood cell magnetic columns connected to a midiMACS™ magnet for removal of any residual white blood cells. This procedure did not induce any qualitative variation in the processed platelets.

Platelet aggregation. Platelet aggregation was monitored using a Chronolog Model 560VS aggregometer with AGGRO/LINK version 5.1.9 software, at a stirring speed of 1000 rpm. Aliquots (200 μL) of PRP were placed in cuvettes containing magnetic stirrer bars, warmed at 37°C, and stirred for 90 seconds to obtain a stable baseline. Platelet concentration in PRP was adjusted to 2×10^8 platelets/ml using platelet poor plasma of the same genotype.

Flowcytometry. Human and murine platelet suspensions (2.5×10^7 /mL) prepared by gel-filtration in modified HEPES-Tyrode buffer (137mM NaCl, 12mM NaHCO₃, 2.5mM KCl, 10mM HEPES, 0.1% BSA, 0.1% Dextrose, 2mM Ca²⁺ and 1mM Mg²⁺, pH 7.4) were incubated with specific blocking agents or controls for 15 minutes at room temperature, followed by stimulation with indicated agonists. Both quiescent and activated platelets were fixed in 1% formaldehyde for 10 minutes. P-selectin expression and integrin- $\alpha_{IIb}\beta_3$ activation were assessed as described previously.⁸ Human or murine specific FITC conjugated anti-TLR9 antibodies were used to estimate the surface expression of TLR9. Data was acquired using a FACS Calibur instrument (Becton Dickinson, San Jose, CA) and analyzed using the FlowJo 9.0.2 software (Tree Star, Ashland, OR).

Immunocytochemistry, Immunohistochemistry, and epi-fluorescence microscopy. Platelets were isolated and incubated with CAPs (10 μ M) for 15 minutes. Subsequently, platelets were spread on glass slides, fixed in 4% formaldehyde for 15 minutes, permeabilized with 0.25% Triton X-100, and blocked in immunofluorescence blocking buffer (1% BSA, in PBST) for 1 hour before antibody labeling. For TLR9 localization, samples were incubated with primary antibodies against human (EMD Millipore) or murine (InVivogen) TLR9 alone or in combination. All samples were treated with respective goat anti-rabbit and/or donkey anti-mouse antibody conjugated to an Alexa Fluor 488 or 568 nm (Invitrogen; Molecular Probes). As background controls, slides were incubated with non-immune IgG and appropriate secondary antibody. All images were adjusted to account for nonspecific binding of antibodies. For colocalization experiments with Rab4, Rab9, and CAPs, platelets were subsequently probed with primary antibodies against TLR9 (EMD Millipore), Rab4, Rab9 (Cell Signaling Technology), and rabbit polyclonal anti-CEP antibody.

For immunohistochemistry, cryosections were warmed at RT for 30 min, fixed in cold acetone or methanol, permeabilized with 0.5% saponin and blocked by 1% BSA + 10% normal goat serum in TBS for 1 hour, and subsequently incubated overnight at 4°C with rabbit polyclonal anti-CEP antibody (1:400) in the blocking buffer.⁹ Samples were washed and exposed to an Alexa Fluor conjugated secondary antibody. Next, the slides were mounted in Vectashild™ with DAPI and examined using Leica epi-fluorescent microscope, equipped with a 60Å~ NA 1.42 Plan-Apochromat 63x/100x oil immersion objective. Images were captured and processed by a cooled CCD camera and Q-Imaging software (QCapture PRO 6.0).

Human TLR9 activation assay in HEK-Blue™ hTLR9 cells. The HEK-Blue™ hTLR9 cells that stably co-express the human TLR9 and an NF- κ B-inducible *SEAP* reporter gene and the control cells HEK-Blue™ Null were cultured in a DMEM, 4.5g/L glucose, 10% (v/v) fetal bovine serum, 50 U/mL penicillin, 50 μ g/mL streptomycin, 100 μ g/mL Normocin™, 2mM L-glutamin, in a flat-bottom 96-well plate and were maintained at 37°C with 5% CO₂ in a humidified incubator. Cells were cultured for 18 hours in the presence of indicated concentrations of agonists, and NF- κ B-induced SEAP activity was assessed in the culture supernatant using QUANTI-Blue™, and a reading at OD 620 nm as per the manufacturer's protocol.

RNA purification and analysis. RNA extraction from platelets was performed using TRI Reagent® (Sigma-Aldrich Corp. St Louis, MO, USA) according to the manufacturer's recommended protocol, and cDNA was synthesized using Superscript III (Invitrogen). These procedures were performed according to the manufacturer's instructions. Negative control reactions were performed for cDNA synthesis in the absence of the Superscript III enzyme. The sequences of the primer pairs used for cDNA quantitation are as follows:

Tlr9 forward (F), 5'-AGGCTGTCAATGGCTCTCAGTT-3',
reverse (R), 5'TGAACGATTTCCAGTGGTACAAGT-3';

Negative control reactions were cycled alongside test samples to ensure the absence of contaminating genomic DNA.

Western blotting and co-immunoprecipitation (CoIP). Human and murine platelets were stimulated with indicated agonists for 15 minutes at 37°C, lysed at 4°C in a lysis buffer containing protease and phosphatase inhibitors, briefly centrifuged, and supernatants were mixed with equal volume of a SDS-PAGE sample buffer containing DTT. Equal amounts of protein (~50µg) were separated on a 4-20% Tris-HCl gradient gel and transferred to PVDF membranes for immunodetection of specific proteins by enhanced chemiluminescence. For the CoIP assay, human leukocyte depleted gel-filtered platelets were pre-cleared with Protein-G beads and then incubated with CEP-BSA for 4 hours at 4°C. CEP-BSA was immunoprecipitated from human platelet lysate by sequential use of anti-BSA antibody and Protein-G beads. Protein G beads were stringently washed, treated with equal volume of a SDS-PAGE sample buffer and a sample was then used for detection of TLR9 by western blotting.

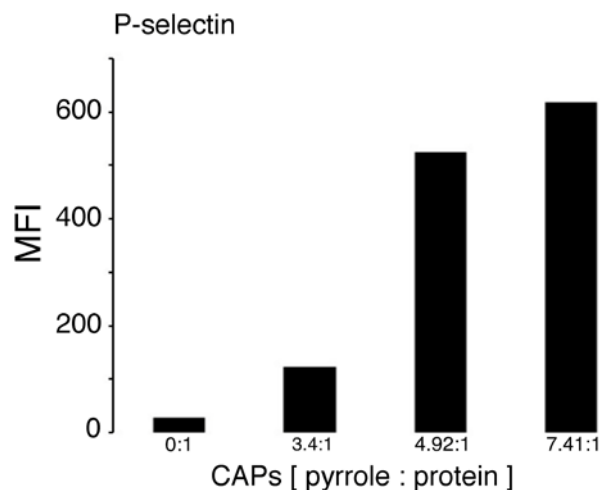
Surface Plasmon Resonance (SPR). Real-time protein-protein interactions were analyzed using a Biacore3000 (BIAcore AB, GE Healthcare). Functional grade TLR9 peptides (Novus Biological) were bound to CM5 biosensor chips (Biacore) according to the manufacturer's instructions at pH 5.5. Experiments were performed at room temperature in a HBS-P (10 mM HEPES, 150mM NaCl, 0.005% surfactant P20) buffer (pH 7.4) with 0.1% BSA at a flow rate of 20 µL/min, allowing 2 minutes of binding and 3 minutes of dissociating time. Analyte binding to the immobilized ligand was recorded by measuring the variation of the SPR angle, and the results are expressed in resonance units (RU).

Intravital Thrombosis. Intravital thrombosis study was performed using an acute carotid artery injury model as previously described.⁸ Isolated murine platelets were labeled with calcein green (Molecular Probes) and injected into the mice (1×10^6 platelets per gram of body weight) via the lateral tail vein. Whatman No.1 filter paper strips ($1.5 \times 1.5 \text{ mm}^2$) soaked with 12% FeCl₃ solution were applied to the surface of the carotid artery for 2 minutes to induce a transmural injury. The time to occlusion was defined as the time from removing the filter paper with FeCl₃ to the time of complete flow cessation lasting for at least 1 minute. The blood vessels were observed under a Leica DM LFS microscope (Leica, Germany) with 10x/0.30 objectives. Images were acquired using a cooled high-speed, digital camera (QImaging Retiga EXi Fast 1394) and with Streampix acquisition software.

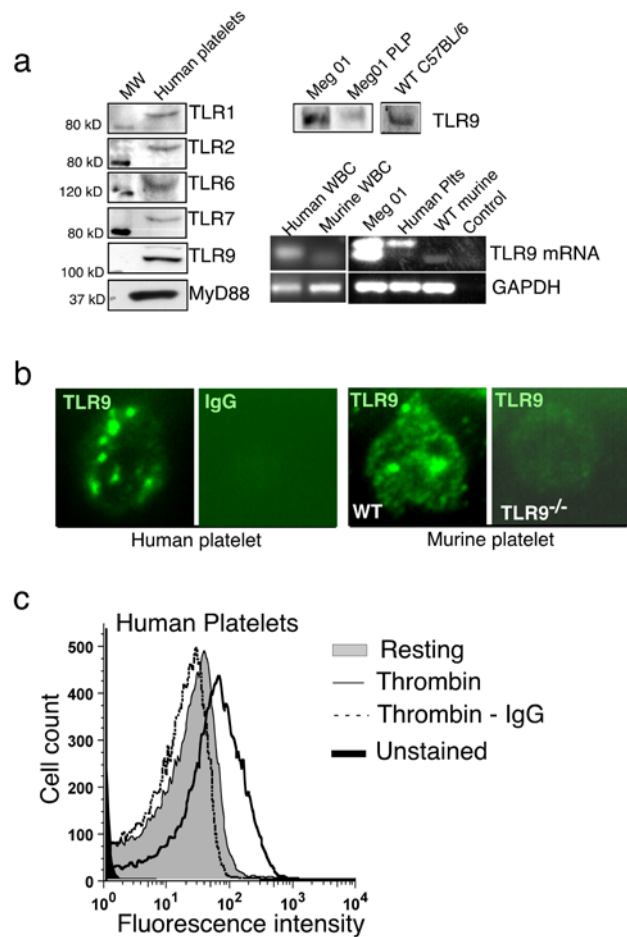
Tail cut bleeding time. Pairs of mice were anesthetized and placed on a pre-warmed pad. Tails were cut with a scalpel at the position where the diameter of the tail was 2.0 mm. Each tail was immersed in normal saline (37°C). The time from the incision to cessation of bleeding was recorded as a data point. (The amount of shed blood was determined by reducing the known volume of saline from the total amount of blood plus saline after the bleeding is completely stopped.)

Statistical analysis. Values are expressed as means \pm standard errors of mean (SEM). The statistical significance was evaluated between two groups of data using a two-tailed unpaired Student's *t* test. We used two-tailed nonparametric Mann Whitney U test for analyzing the results of 'intravital carotid thrombosis', and 'tail cut bleeding time' studies. The *p* values less than 0.05 were considered as statistically significant.

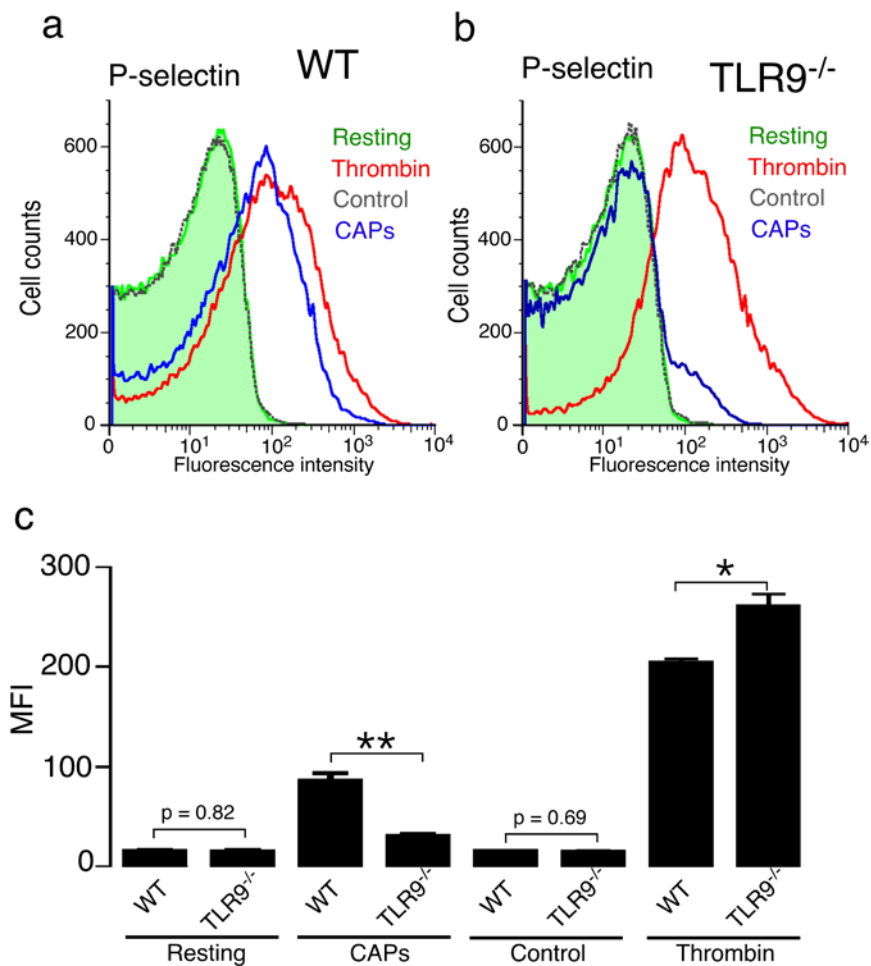
II. Supplementary Figures



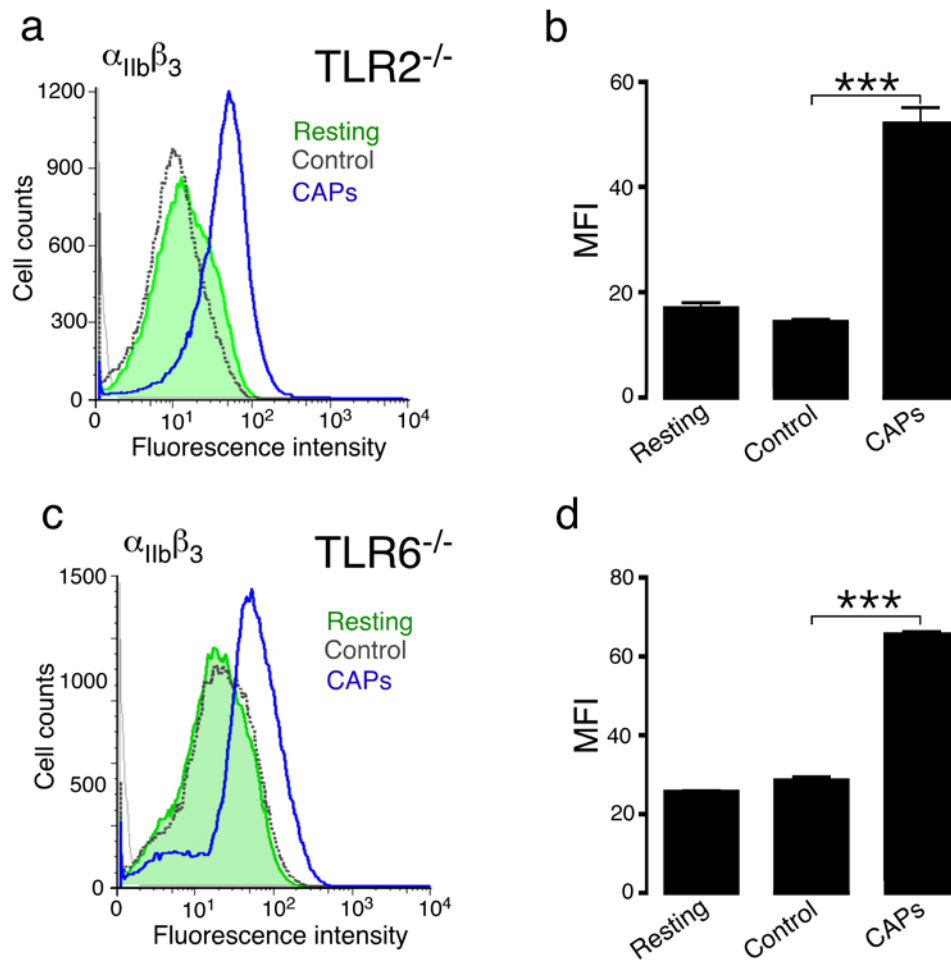
Online Figure I. CAPs induced platelet activation depends on the extent of protein modification. Carboxyethyle-pyrrole (CEP) adducts of bovine serum albumin (BSA) were prepared at an ascending pyrrole to protein molar ratio and the efficiency of CAPs (BSA 1.5 μ M with indicated molar ratio of CAPs) to induce P-selecting expression in human platelets, were tested by flowcytometry as described in Methods. Representative bar diagram of mean fluorescence intensities (MFI) of respective groups are shown.



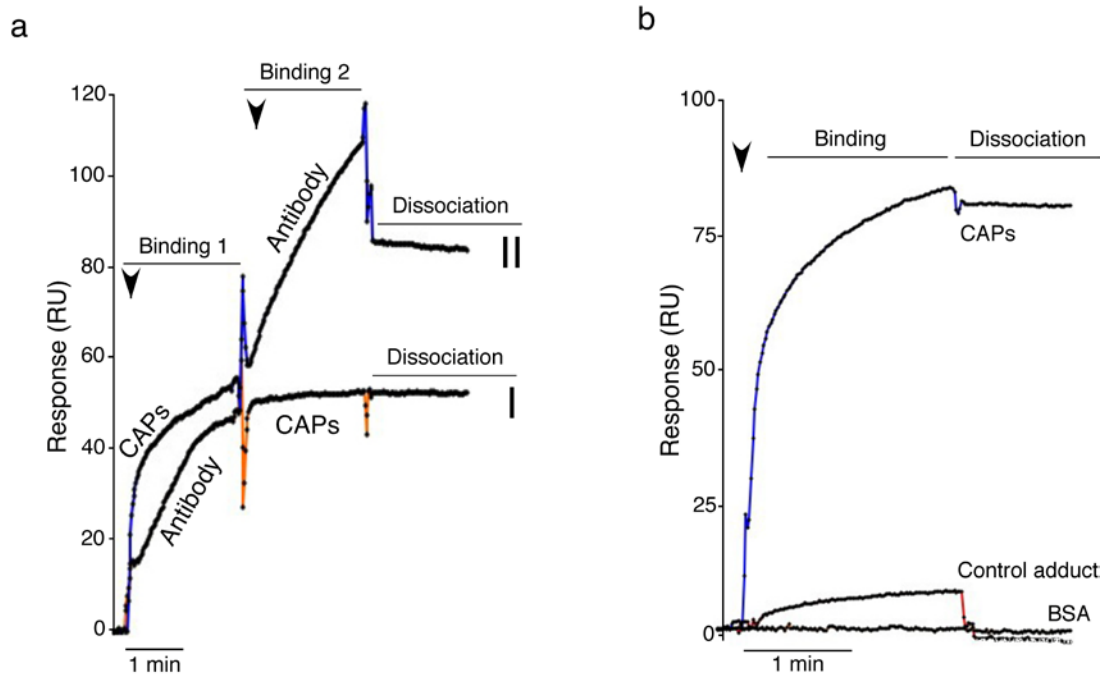
Online Figure II. Human and murine Platelets express Toll-like receptors. Platelet rich plasma was depleted of possible leukocyte contamination, and (a) TLR1, TLR2, TLR6, TLR7, TLR9 and MyD88 were detected by immunoblotting in human platelets; TLR9 in megakaryocyte cell line Meg-01, Meg-01 derived platelet like particle (PLP) and in WT murine platelets. We also detected moderate levels of TLR9 mRNA expression in human and murine platelets by RT-PCR. (b) Human, WT, and TLR9^{-/-} murine platelets at resting state, were fixed with 4% paraformaldehyde on glass slides, permeabilized with 0.25% Triton X-100, and probed for TLR9. Representative image of single platelets revealed distinct localization of TLR9. Cells were viewed in a Leica epi-fluorescent microscope with a Plan-Apochromat 63x, NA 1.4 oil immersion objective and an optical zoom of 10 \times . (c) Detection of increased TLR9 expression by FACS in either resting or α -thrombin activated human platelets, prepared by gel filtration.



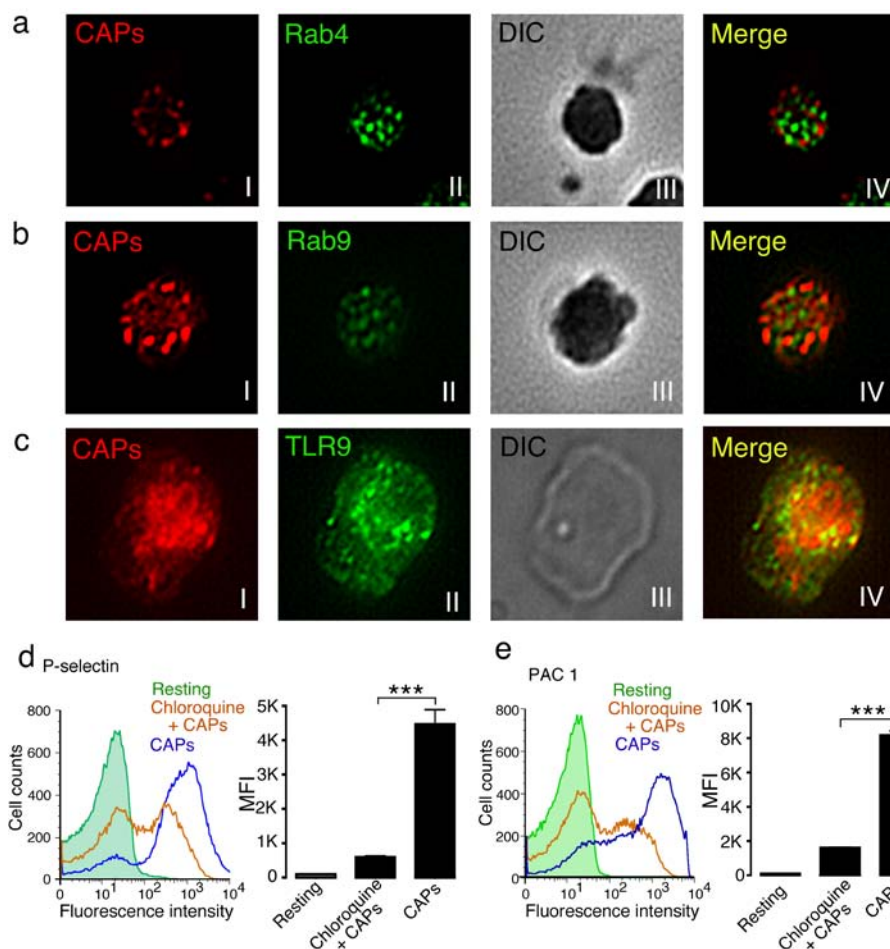
Online Figure III. Carboxy-alkyl-pyrrole protein adducts induce P-selectin expression in murine platelets in a TLR9 dependent manner. Platelets from a. wild type, and b. TLR9 knockout mice were isolated by gel filtration and stimulated with α -thrombin (0.05U/mL), CAPs (albumin 1.5 μ M, pyrrole 12.5 μ M) and P-selectin expression was assessed by flowcytometry. c. Quantification of the mean fluorescence intensity (MFI) values, presented as mean (SEM). N = 3. * p<0.02, ** p<0.002



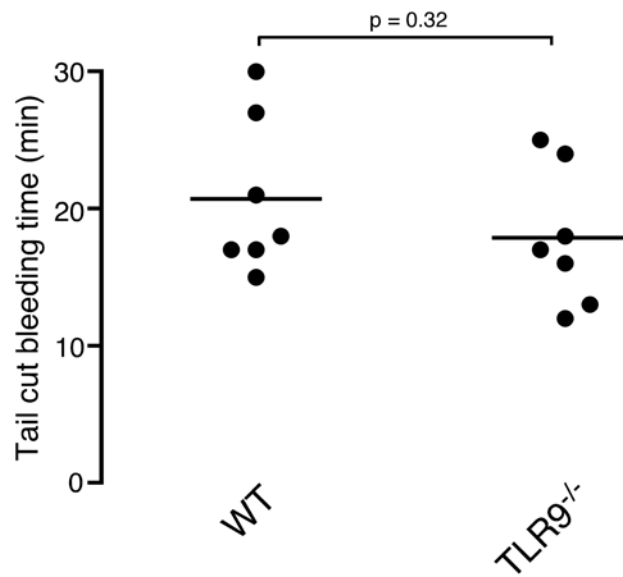
Online Figure IV. Carboxy-alkyl-pyrrole protein adducts induce platelet integrin activation in TLR2 and TLR6 deficient murine platelets. Platelets from a. TLR2, and b. TLR6 knockout mice were isolated by gel-filtration and stimulated with CAPs (albumin 1.5 μ M, pyrrole 12.5 μ M) and integrin- $\alpha_{IIb}\beta_3$ activation was assessed by FACS using JON/A antibody. Right panels show quantification of the mean fluorescence intensity (MFI) values presented as mean (SEM). N = 3. *** p<0.0001.



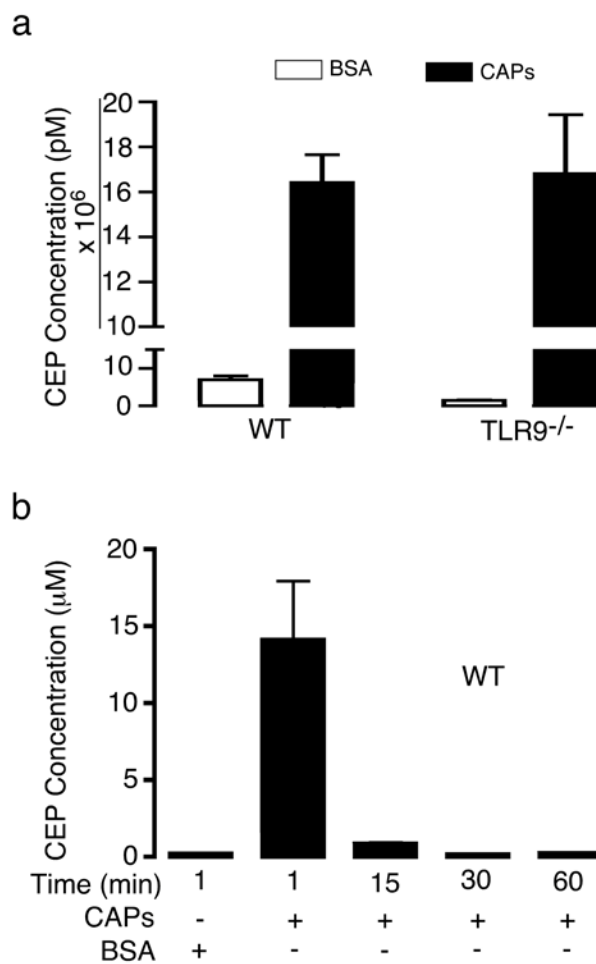
Online Figure V. The direct interaction and stable binding of CAPs is specific to Toll-like receptor 9. *Surface plasmon resonance (SPR):* The real-time protein-protein interactions and binding response were recorded as ‘resonance unit’ (RU) using a Biacore3000 (Biacore AB, GE Healthcare) SPR system. (a) *Co-injection assay:* CAPs with a 9.3:1 pyrrole-protein ratio and functional TLR9 monoclonal antibody (mAb) targeting the leucine rich regions (LRR) of TLR9 were injected sequentially at a flow rate of 20 $\mu\text{L}/\text{min}$, to flow through a CM5 biosensor chip coated with functional TLR9 peptide. The binding and dissociation curves were recorded over time. I. Functional grade blocking TLR9 mAb to cover the receptor binding sites (Binding 1), followed by CAPs (Binding 2) were injected for a period of 2 minutes each and 3 minutes were allowed for dissociation. II. In the control experiment, CAPs (Binding 1), and then the blocking TLR9 mAb (Binding 2) was injected in the same fully regenerated CM5 chip. (b) The TLR9 binding of a non-CEP control adduct of BSA was compared to that of CAPs (CEP-BSA) using the same completely regenerated CM5 biosensor chip and identical instrument settings.



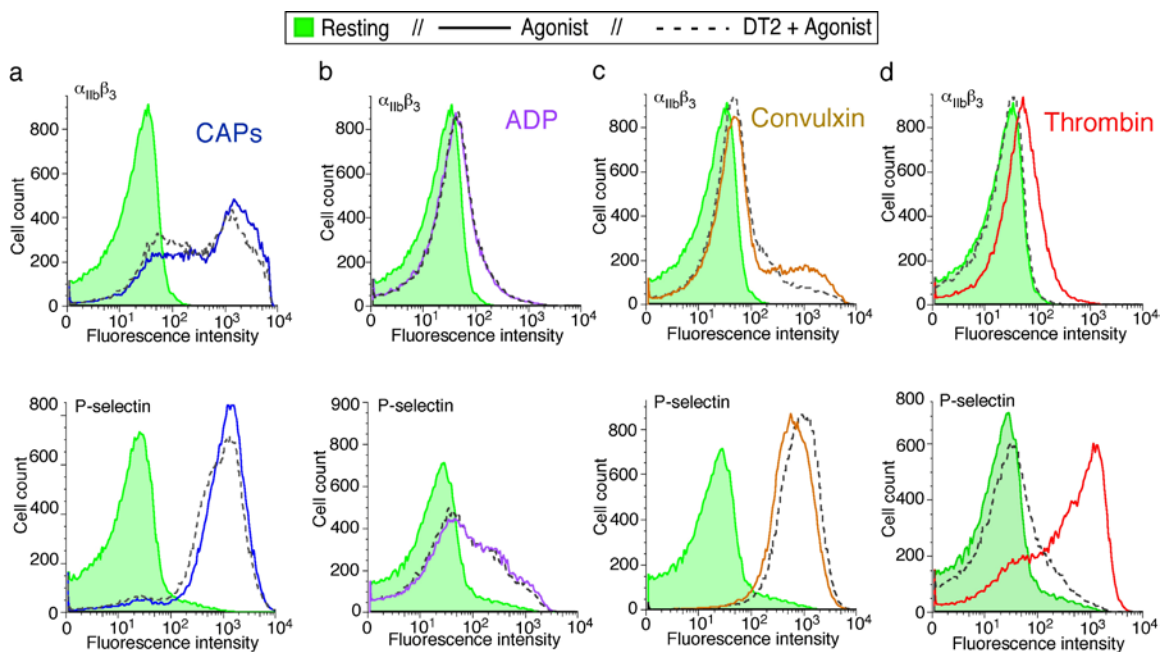
Online Figure VI. CAPs is present not in early but in the late endosomes, co-localize with TLR9 and induce platelet activation in an endosomal pH dependent manner. (a-c) *Co-immunofluorescence*: Using multi-chamber slides, human platelets prepared by gel filtration (GFP), were incubated with CAPs (10 μ M of pyrrole) and co-stained with two primary antibodies and corresponding fluorochrome conjugated secondary antibodies against, (a) I. CAPs, and II. Rab4; (b) I. CAPs, and II. Rab9; (c) I. CAPs, and II. TLR9, as described in the methods. III. Representative DIC images of platelets. IV. Merged color images are shown in the right most columns. (d-e) *Activation of human GFP by CAPs in presence or absence of the endosomal acidification inhibitor chloroquine*: Human GFP was preincubated with Chloroquine (20 μ M) for 30 min at 37°C. CAPs (10 μ M of pyrrole) induced (d) P-selectin expression, and (e) integrin $\alpha_{IIb}\beta_3$ (PAC1) activation were assessed. Representative flowcytometry histograms are shown in the left panels. Quantifications of the data as mean fluorescence intensity (MFI) values (SEM) are shown in the respective right panels. N =3, *** p<0.0001.



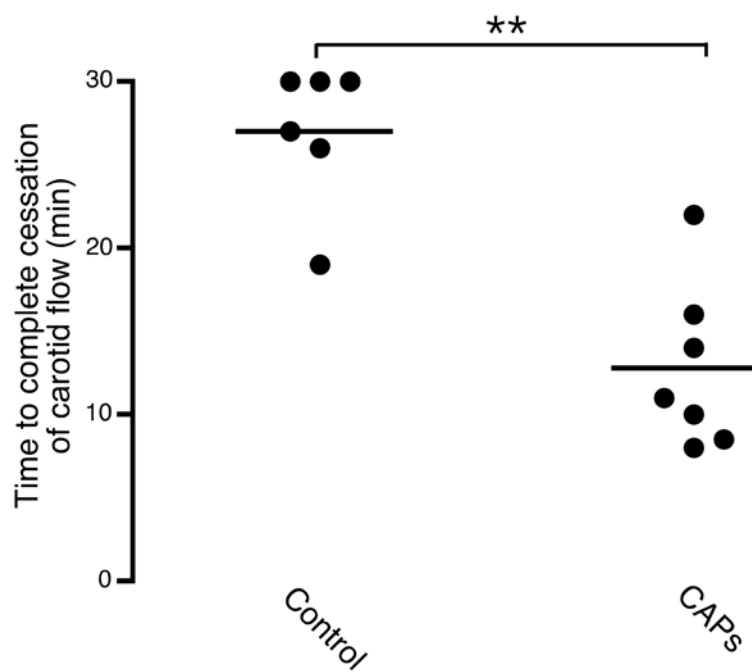
Online Figure VII. Tail cut bleeding time is unaffected by TLR9 deficiency. Age and sex matched WT and TLR9 null mice were anesthetized in pairs, then their tails were amputated at a position where the diameter of the tail was 2.0 mm and immersed in saline at 37°C. The time from the amputation to complete cessation of bleeding was recorded. The difference between groups of mice was analyzed using nonparametric Mann-Whitney test. N = 7, Two-tailed p = 0.32.



Online Figure VIII. Measurement of CEP in WT and TLR9^{-/-} mice after intravenous administration of CAPs (CEP-BSA). a. WT and TLR9^{-/-} were injected intravenously with BSA or CEP-BSA (~20μM) and plasma CEP levels were measured immediately after the injection by competitive ELISA as described in the Methods section. b. CEP-BSA (20μM) was injected intravenously in WT mice, and plasma CEP levels were measured by competitive ELISA at 1, 15, 30, and 60 minutes. Quantifications of the data are presented as histograms of mean values (SEM). N =3.

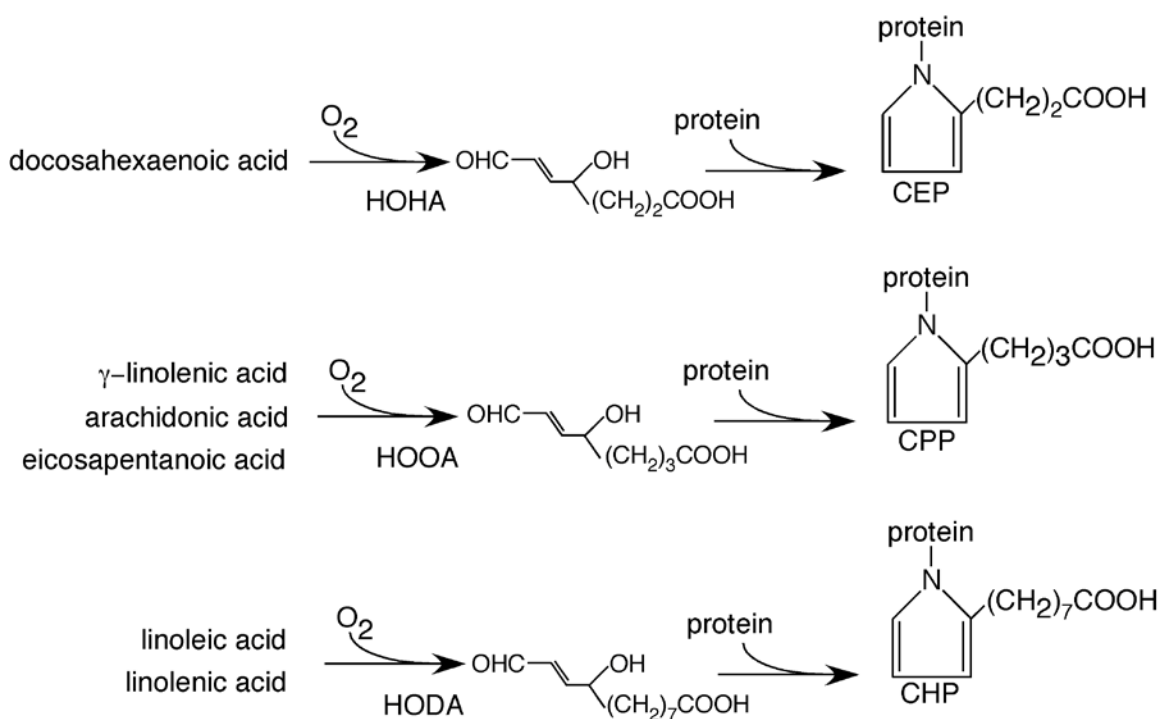


Online Figure IX. Effects of the inhibitor cGMP dependent protein kinase on CAPs induced activation of human platelets. Human platelets isolated by gel-filtration were incubated with 100nM of DT2 followed by stimulation with CAPs, ADP 10 μ M, Convulxin 100 ng/mL, or thrombin 0.005 U/mL. Integrin $\alpha_{IIb}\beta_3$ activation (upper row) and P-selectin expression (lower row) were assessed by flowcytometry.



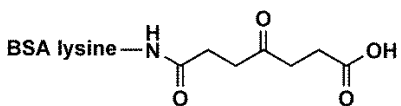
Online Figure X. Carboxy-alkyl pyrrole protein adducts induce accelerated thrombosis in TLR2^{-/-} mice. Age and sex matched TLR2^{-/-} null mice were anesthetized, injected with CAPs (albumin 1.2 μ M, Pyrrole 10 μ M) or sham-modified control albumin (1.2 μ M) as described in Methods, carotid arteries were exposed and thrombosis induced by application of FeCl₃. Thrombus formation in carotid arteries was visualized and the time to complete thrombotic occlusions were recorded. Data was analyzed by two-tailed nonparametric Mann Whitney test. ** p < 0.003.

Supplemental Tables



Online Table I. Schematic diagrams of carboxyalkylpyrrole protein adduct (CAPs) biogenesis.

HOHA	-4-hydroxy-7-oxohept-5-enoic acid
CEP	-2-(ω -carboxyethyl)pyrrole
HOOA	-5-hydroxy-8-oxooct-6-enoic acid
CPP	-2-(ω -carboxypropyl)pyrrole
HODA	-9-hydroxy-12-oxododec-10-enoic acid
CHP	-2-(ω -carboxyheptyl) pyrrole

Table I	
Acetylated BSA	OHdiA-BSA
	
Caproylated BSA	Maleylated BSA
Undecanoylated BSA	Succinylated BSA
Palmitoylated BSA	Adipoylated BSA
Suberoylated BSA	(Acetic acid glycol monoester)-Glutaryl-BSA
Dodecanedioylated BSA	(Choline phosphate glycol monoester)-Glutaryl-BSA
PGPC-BSA	(Palmitic acid glycol monoester)-Glutaryl-BSA

Protein-adducts formed by oxidized lipids, which resembled hydroxy- ω -oxoalkenoic acids but not capable of forming pyrroles were used in some of the platelet activation assay to compare the specificity of platelet activation property of 2-(ω -carboxyalkyl)pyrrole protein adducts. None of such protein adducts tested, and shown above, had any direct or indirect effect on platelet activation in our *in vitro* experiments.

Supplemental References

1. Febbraio M, Abumrad NA, Hajjar DP, Sharma K, Cheng W, Pearce SF, Silverstein RL. A null mutation in murine cd36 reveals an important role in fatty acid and lipoprotein metabolism. *J Biol Chem*. 1999;274:19055-19062
2. Gu X, Meer SG, Miyagi M, Rayborn ME, Hollyfield JG, Crabb JW, Salomon RG. Carboxyethylpyrrole protein adducts and autoantibodies, biomarkers for age-related macular degeneration. *J Biol Chem*. 2003;278:42027-42035
3. Kaur K, Salomon RG, O'Neil J, Hoff HF. (carboxyalkyl)pyrroles in human plasma and oxidized low-density lipoproteins. *Chem Res Toxicol*. 1997;10:1387-1396
4. Gu X, Sun M, Gugiu B, Hazen S, Crabb JW, Salomon RG. Oxidatively truncated docosahexaenoate phospholipids: Total synthesis, generation, and peptide adduction chemistry. *J Org Chem*. 2003;68:3749-3761
5. Smith PK, Krohn RI, Hermanson GT, Mallia AK, Gartner FH, Provenzano MD, Fujimoto EK, Goeke NM, Olson BJ, Klenk DC. Measurement of protein using bicinchoninic acid. *Anal Biochem*. 1985;150:76-85
6. DeCaprio AP, Jackowski SJ, Regan KA. Mechanism of formation and quantitation of imines, pyrroles, and stable nonpyrrole adducts in 2,5-hexanedione-treated protein. *Mol Pharmacol*. 1987;32:542-548
7. Sayre LM, Sha W, Xu G, Kaur K, Nadkarni D, Subbanagounder G, Salomon RG. Immunochemical evidence supporting 2-pentylpyrrole formation on proteins exposed to 4-hydroxy-2-nonenal. *Chem Res Toxicol*. 1996;9:1194-1201
8. Podrez EA, Byzova TV, Febbraio M, Salomon RG, Ma Y, Valiyaveetil M, Poliakov E, Sun M, Finton PJ, Curtis BR, Chen J, Zhang R, Silverstein RL, Hazen SL. Platelet cd36 links hyperlipidemia, oxidant stress and a prothrombotic phenotype. *Nat Med*. 2007;13:1086-1095
9. Crabb JW, Miyagi M, Gu X, Shadrach K, West KA, Sakaguchi H, Kamei M, Hasan A, Yan L, Rayborn ME, Salomon RG, Hollyfield JG. Drusen proteome analysis: An approach to the etiology of age-related macular degeneration. *Proc Natl Acad Sci U S A*. 2002;99:14682-14687